Comparing Leakage Matrices

tim larson and Jesper Schou
Stanford University

Sylvain Korzennik
Harvard-Smithsonian Center for Astrophysics

contact: tplarson@sun.stanford.edu

The standard leakage matrix for global mode helioseismology is calculated assuming a value of zero for the P-angle, B-angle, and CCD offsets, and value of 1 AU for the observer distance. Since image center is not constant we vary this parameter so see what effect is has on the leaks and explore the possibility of using a leakage matrix averaged over pixel offsets. Since the B-angle and observer distance vary in a known way with time, we recompute the leakage matrix for realistic values of these parameters and repeat the fits to find out how the mode parameters are affected. Since previous studies have indicated certain systematic errors are associated with the apodization, we also compute leakage matrices for different apodizations, repeat the spherical harmonic decomposition with those apodizations, and fit these to see the effect on mode parameters. Lastly, we compare the leakage matrix computed at Stanford with a completely independent calculation in order to both verify our results and discover the source of any discrepancy.

Overview of Global Pipeline

1. Apodize dopplergrams in image radius.
2. Remap to uniform grid in longitude and sin(latitude).
3. Fourier transform in longitude, take inner product in latitude with associated legendre functions.
4. Form timeseries of resulting spherical harmonic coefficients, detrend and fill gaps.
5. Fit peaks in the fourier transform of these, taking leaks into account.

The leaks are the result of geometry; because we can only see somewhat less than half of the Sun, the inner product in step 3 cannot perfectly separate the modes. These leaks then appear as additional peaks in the power spectrum of the target mode.

Problems

MDI provides two types of data commonly used for global helioseismology: full disk and vector weighted. The full disk data is generally of higher quality but due to telemetry constraints is only available a few months of each year. The vector weighted data, so called because it is convolved with a gaussian “vector”, has a much better duty cycle, but it is also subsampled by a factor of 5 and highly apodized. One might naively hope that the inferences drawn from these two datasets might be in agreement with each other.

Unfortunately, and as the plots below show, this is not the case. The top plots show the normalized residuals for one of the a-coefficients. If the model is a good fit to the data, we would expect for these to be normally distributed around zero. The feature seen in the vector weighted data at 3.4 mHz is an unexplained deviation from this, but it is almost completely absent in the full disk data.

The bottom plots below show rotation profiles obtained from RLS inversions. Again, the vector weighted data show a spurious feature, the polar jet. And again, it is absent in the full disk data.

Our previous investigations have revealed that both of these features depend more strongly on the apodization of the data rather than its resolution. We therefore began to suspect that there could be errors in the leakage matrix.

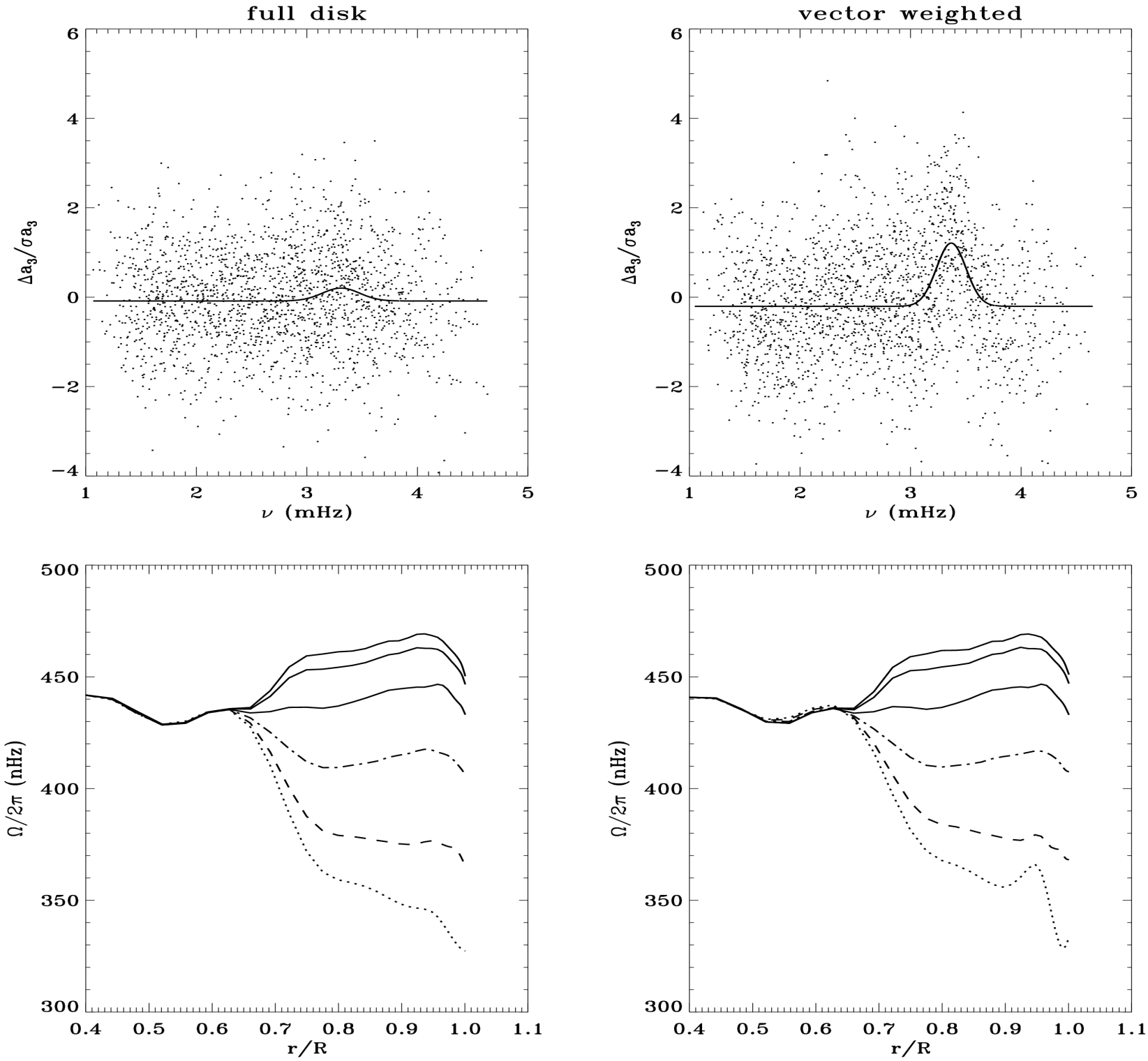
full disk
vector weighted
$\Delta a_3/\sigma a_3$
ν (mHz)
$\Omega/2\pi$ (nHz)
r/R

How to Make a Leakage Matrix

We begin by generating fake spherical harmonic images with a given P-angle, B-angle, observer distance, and CCD offsets. For all of our previous work, a value of 1 AU was used for the observer distance and a value of zero was used for the rest. After projecting onto the line of sight, we have the option of convolving the image with a point spread function (PSF). If we are calculating the images at high enough resolution, we can also bin them during this step. Because the PSF of MDI is not well known, the full disk images are left as they are. For vector weighted images we convolve with a gaussian, but in the past we have not subsampled the images. Rather we have simulated the effect of the interpolation done in the spherical harmonic transform by convolving with the cubic convolution kernel used in the interpolation. The reasons for doing this will be made clearer below.

Once we have the fake images, they are run through a spherical harmonic decomposition using exactly the same pipeline as used for real data, the results of which have only to be retabulated to yield the leakage matrix. Because of the computational burden, we usually only calculate a subset of all the leaks in this manner, and interpolate the rest.

This process must be done separately for the vertical and horizontal components of the leakage matrix, and in principle for the real and imaginary part of each one of these. One might think that we would have to calculate how the real parts leak into the imaginary parts and vice versa, but these components can often be assumed to be identically zero. The justification for this assumption, as well as where it breaks down, are shown below.

The following equations show a mathematical derivation of the leakage matrix. The observed timeseries for a given l,m is given by taking the inner product with the observed velocity, expressed as a sum over normal modes, with a suitable mask, which incorporates the line of sight projection, the apodization, and the target spherical harmonic.

$$o_{l,m}(t) = \int_{-1}^{1} \int_{-\pi/2}^{\pi/2} V_{\mathrm{obs}}(\phi, x, t) M_l^m(\phi, x) \mathrm{d}\phi \mathrm{d}x$$

$$
\begin{aligned}
&= \int_{-1}^{1} \int_{-\pi/2}^{\pi/2} \sum_{n',l',m'} V_{n',l',m'}(\phi, x, t) M_l^m(\phi, x) \mathrm{d}\phi \mathrm{d}x \\
&= \sum_{n',l',m'} \int_{-1}^{1} \int_{-\pi/2}^{\pi/2} \Big\{ P_{l'}^{m'}(x) \mathrm{Re}(a_{n'l'm'}(t) \mathrm{e}^{\mathrm{i}m'\phi}) \\
&\quad \sqrt{1-r^2}\mathrm{Ap}(r) \frac{1}{\pi} Y_l^m(\theta, \phi) \Big\} \mathrm{d}\phi \mathrm{d}x \\
&= \sum_{n',l',m'} \int_{-1}^{1} \int_{-\pi/2}^{\pi/2} \Big\{ \frac{1}{\pi} P_{l'}^{m'}(x) P_l^m(x) \\
&\quad [\mathrm{Re}(a_{n'l'm'}(t)) \cos(m'\phi) \\
&\quad - \mathrm{Im}(a_{n'l'm'}(t)) \sin(m'\phi)] \\
&\quad [\cos(m\phi) + \mathrm{i} \sin(m\phi)] \sqrt{1-r^2}\mathrm{Ap}(r) \Big\} \mathrm{d}\phi \mathrm{d}x
\end{aligned}
$$

$$
\begin{aligned}
&= \sum_{n',l',m'} \int_{-1}^{1} \int_{-\pi/2}^{\pi/2} \Big\{ P_l^m(x) P_{l'}^{m'}(x) \mathrm{Ap}(r) \\
&\sqrt{1-r^2} \left[\mathrm{Re}(a_{n'l'm'}(t)) \cos(m\phi) \cos(m'\phi) \right. \\
&\left. - \mathrm{Im}(a_{n'l'm'}(t)) \sin(m\phi) \sin(m'\phi) \right] \Big\} \frac{1}{\pi} \mathrm{d}\phi \mathrm{d}x \\
&= \sum_{n',l',m'} \Big\{ c_{l,m,l',m'} \mathrm{Re}(a_{n',l',m'}(t)) \\
&- \mathrm{i} c'_{l,m,l',m'} \mathrm{Im}(a_{n',l',m'}(t)) \Big\} \ .
\end{aligned}
$$

Here the matrix c gives the leakage from the real part of the leak to the real part of the target and the matrix c′ the leakage between the imaginary parts. The other components have been set to zero because for an apodization function that is symmetric around the central meridian, the cos(m′φ)sin(mφ) and sin(m′φ)cos(mφ) terms are odd functions and therefore integrate to zero. For the full disk data this assumption is valid, but for subsampled data it breaks down at high l, because the subsampling is in general not symmetric around the central meridian.

To investigate the effect of our various assumptions, we generated many new medium-l leakage matrices (resolution 204x204). For the sake of brevity, all the results shown below are for the real part of the vertical component only. Furthermore, we show only the values for $\Delta l=\Delta m=0$, in other words the sensitivity to the target mode. The leaks were not interpolated.

Shown first is the default leakage matrix used for medium-l fitting, calculated as described above. Next shown is the effect of using images with the same resolution as the data, as well as the effect of nonzero pixel offsets. As l increases, we violate the Nyquist theorem worse and worse, especially near the limb. The effect is that the leaks calculated have an increased sensitivity to how the pixels line up with the fake spherical harmonics. But we know that the pixel coordinates of image center varies from image to image, so at the outset it would seem impossible to calculate meaningful leaks at high l. The best one might hope for would be to calculate the average over the possible values of x0 and y0. As it turns out, the variation of the leakage matrix with pixel offset seems to vary sinusoidally with a period of 1 pixel. Therefore the average of the sinusoid can be found by averaging the values at 0 pixel and 0.5 pixel offsets, as shown below. In the future, we hope to use a leakage matrix averaged in this fashion.

This is why in the past the vector weighted leakage matrix has been made using full resolution images, because with subsampled images the Nyquist theorem is violated at much lower values of l. On the other hand, we can in principal improve the high l leaks by calculating the fake images at higher resolution.

The next plot shows the magnitude of the real to imaginary leaks when using the medium-l resolution and the same subsampling grid used by MDI.

original leakage matrix, m=l

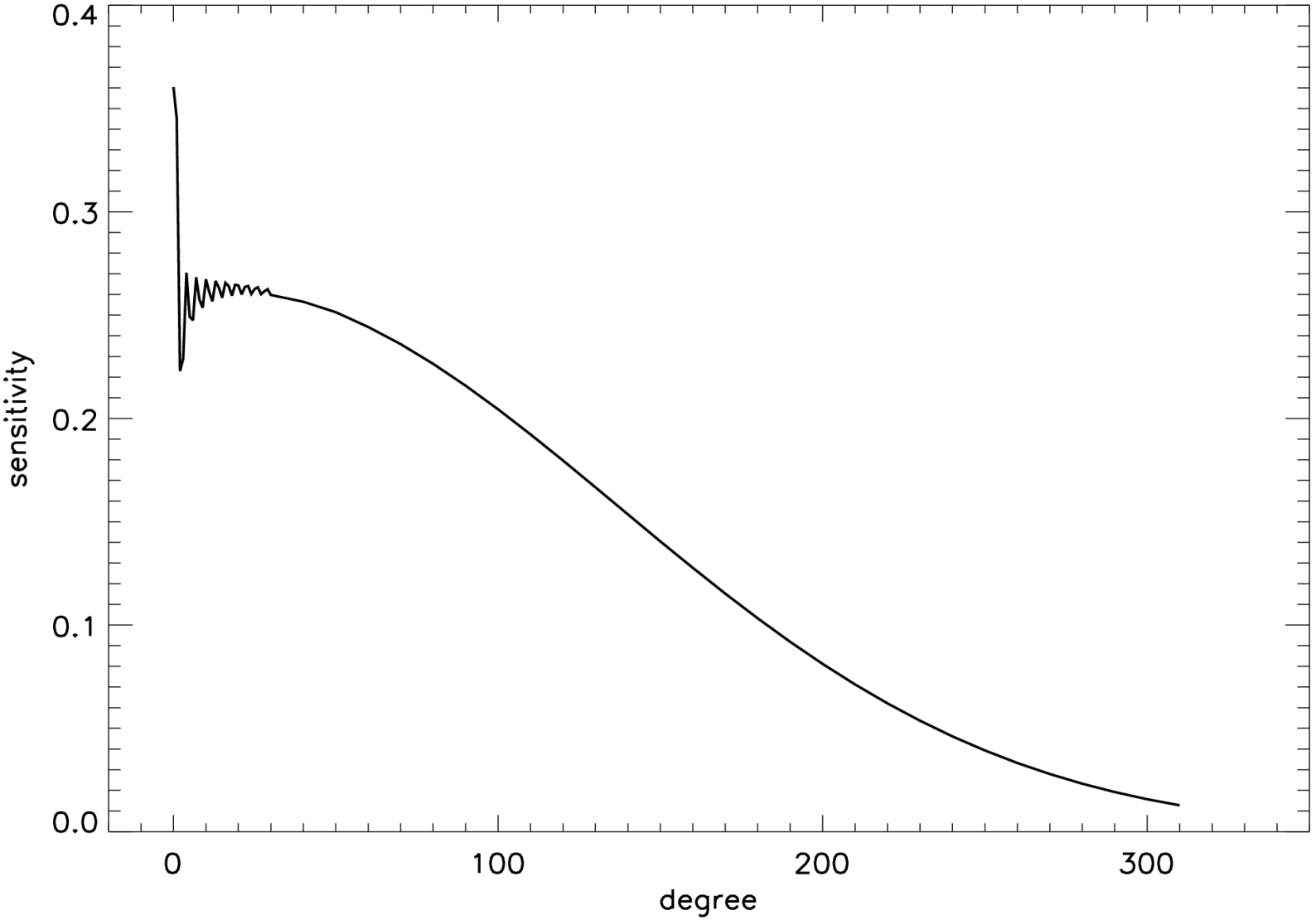

original, medium-l resolution with 0 pixel offset, and medium-l resolution with 0.5 pixel offset in x direction, m=l

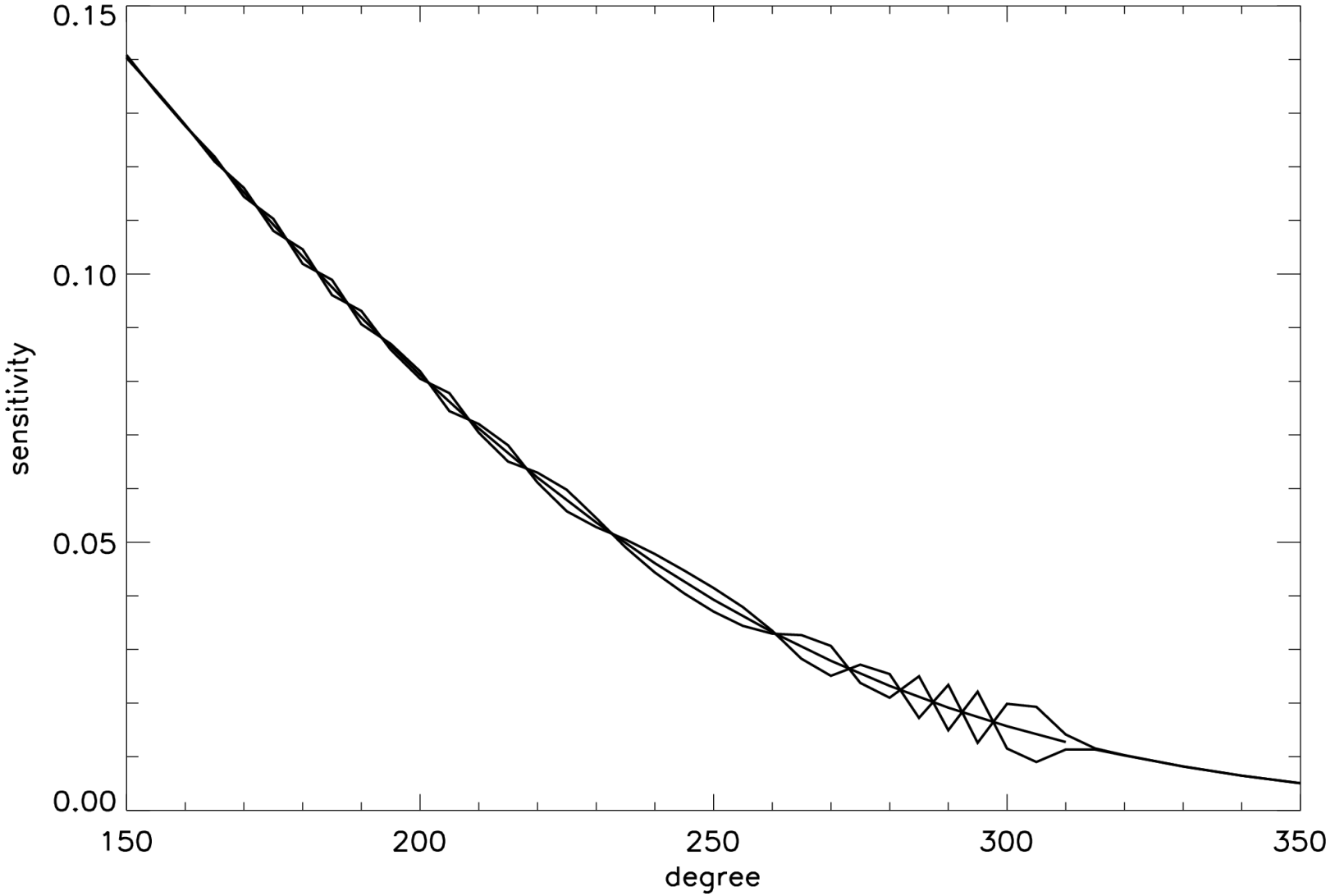

real to imaginary component, m=l

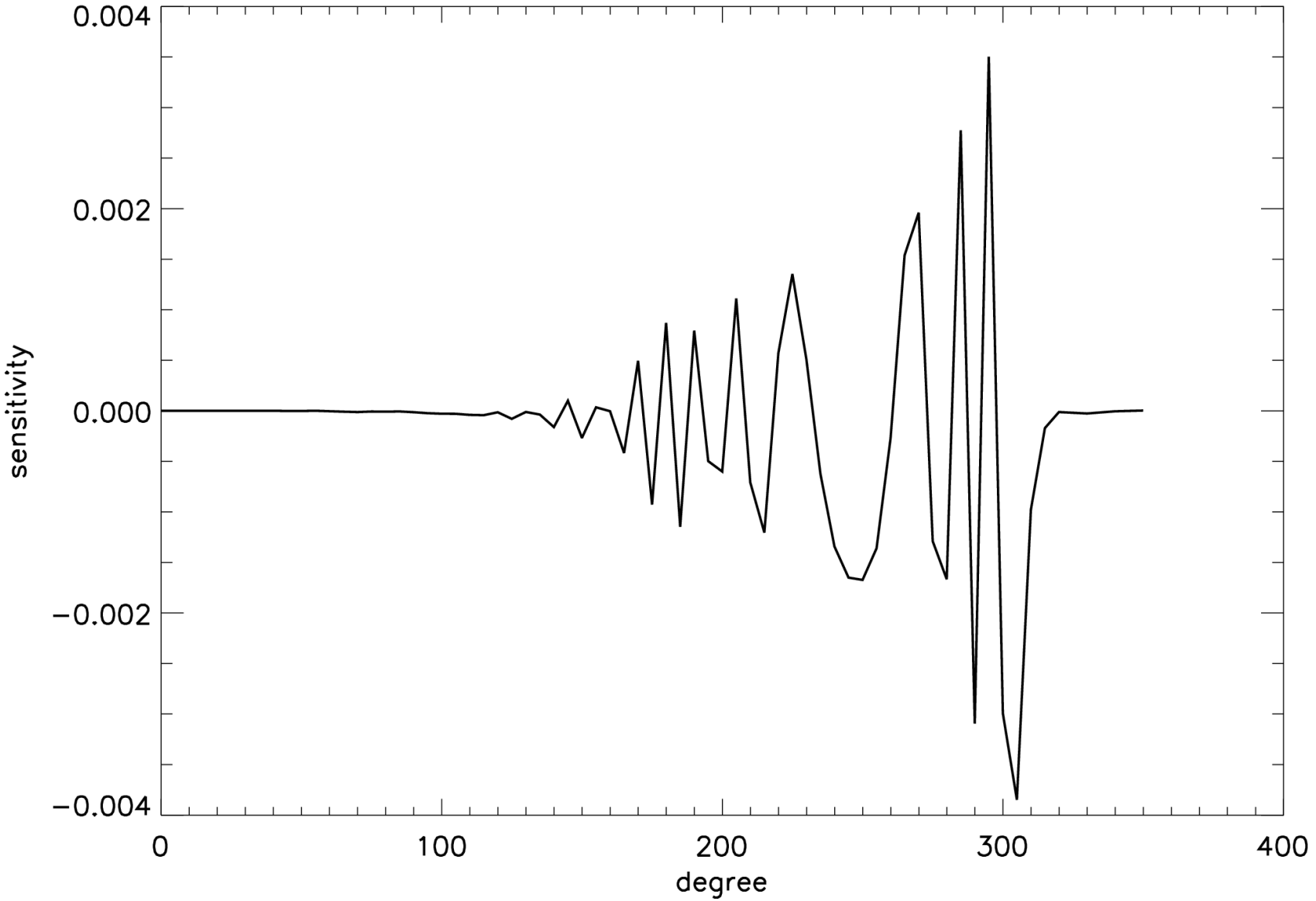

The next two plots show the effect on the leaks of observer distance, which varies from 0.83 to 1.17 AU, and B-angle, which varies in absolute value from 0 to 7 degrees. The B-angle seems to be the only variation that affects the leaks at low l. To check how these differences in the leakage matrix would affect the mode parameters, we found periods with extreme values of observer distance and B-angle, and fitted them with a leakage matrix calculated for those values and one calculated with default parameters. For the observer distance, this had little effect on the mode frequencies, but mode amplitudes were affected by several sigma. For the B-angle, however, the a-coefficients and the inversions based on them showed suggestive differences, as the following two plots show. First shown is the effect of the change in leakage matrix on a_3. In the next plot, the solid line is the inversion corresponding to the default leakage matrix, while the dashed line is for a leakage matrix calculated with an appropriate value for the B-angle. Although the bulk of the polar jet has disappeared, there is still the anomalous upturn near the surface.

max (bottom) and min (top) observer distance, m=l

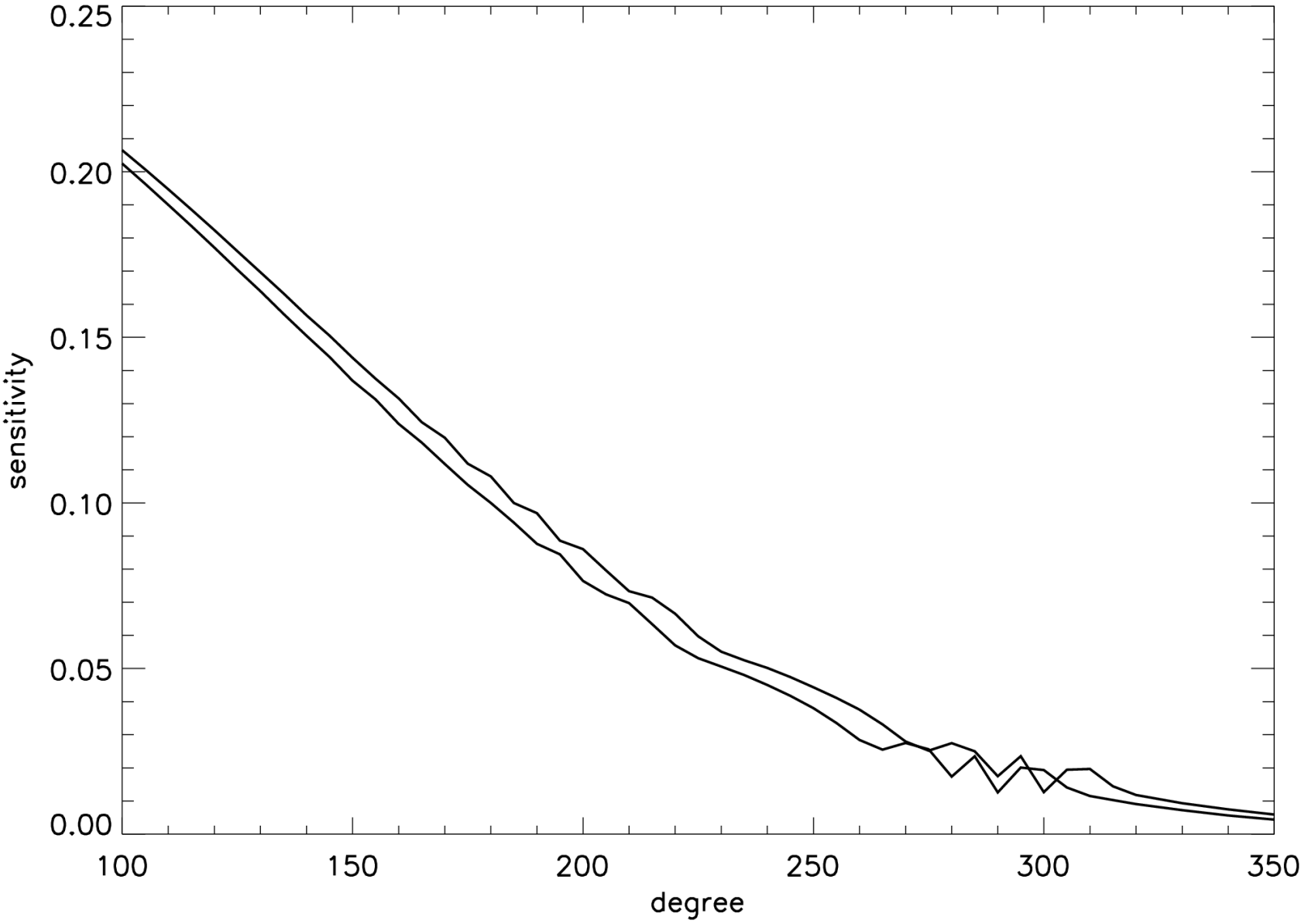

B-angle = 0 (solid) and B-angle = 7 (dashed), m=0

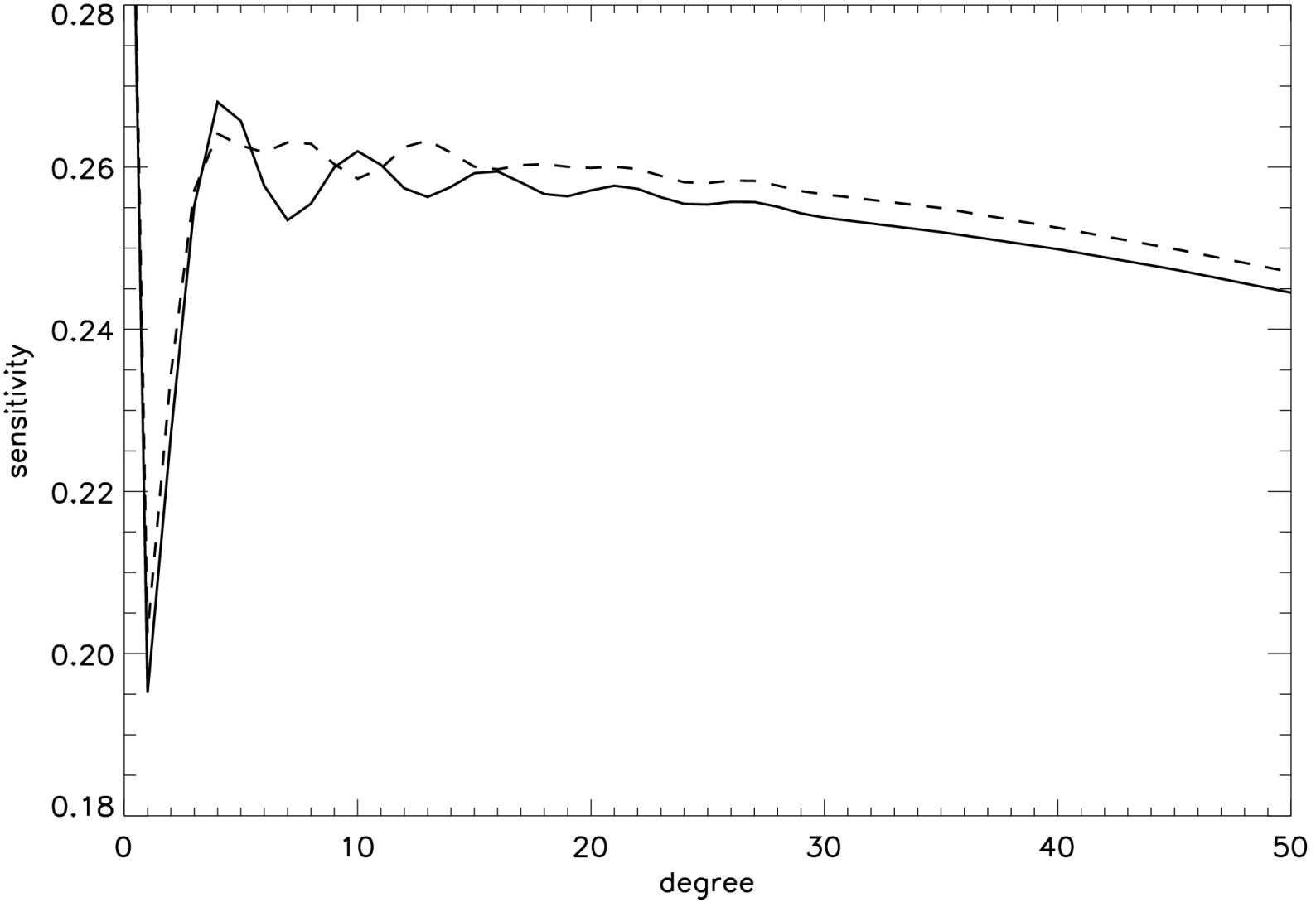

effect of B-angle

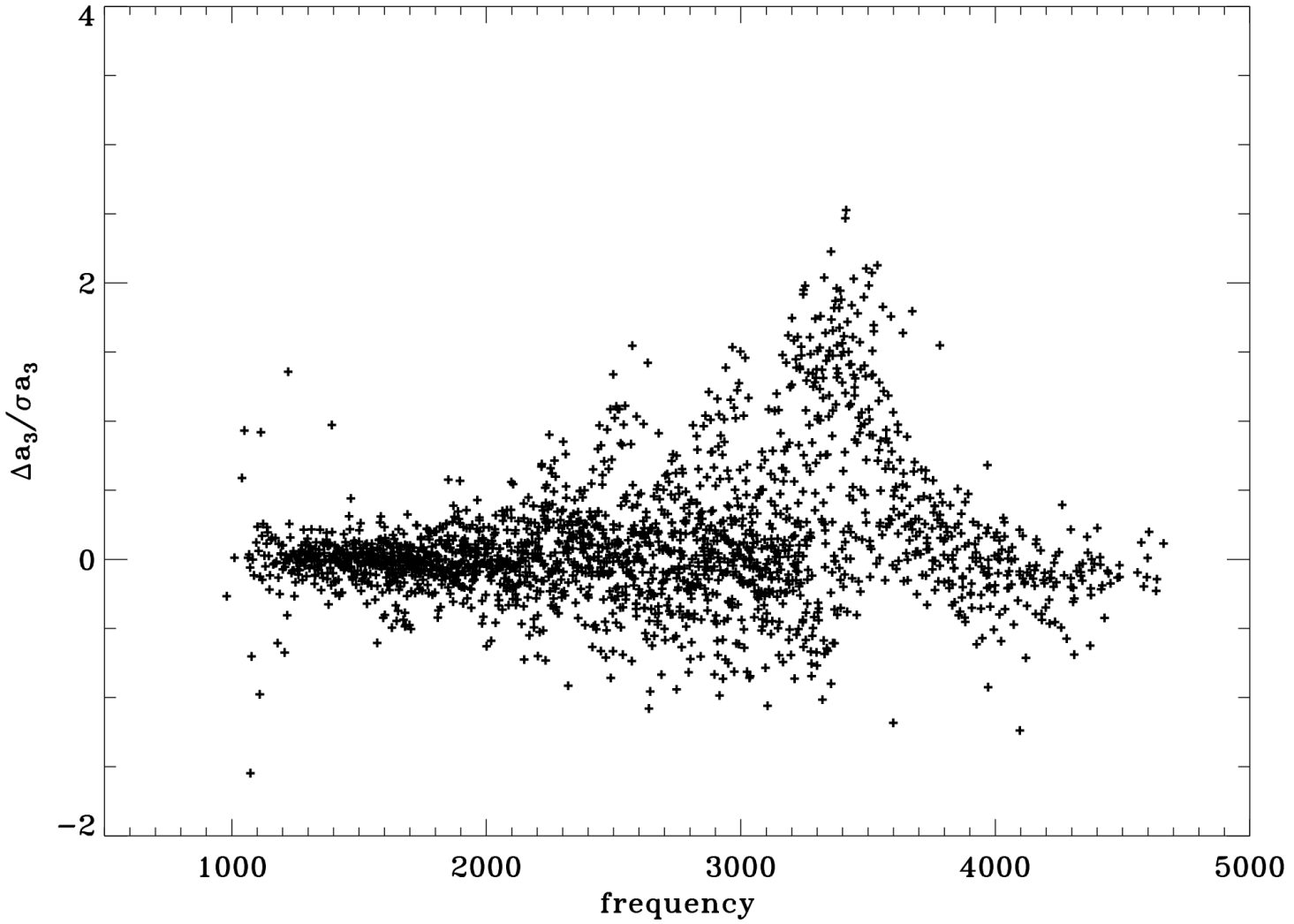

internal rotation at 75 deg

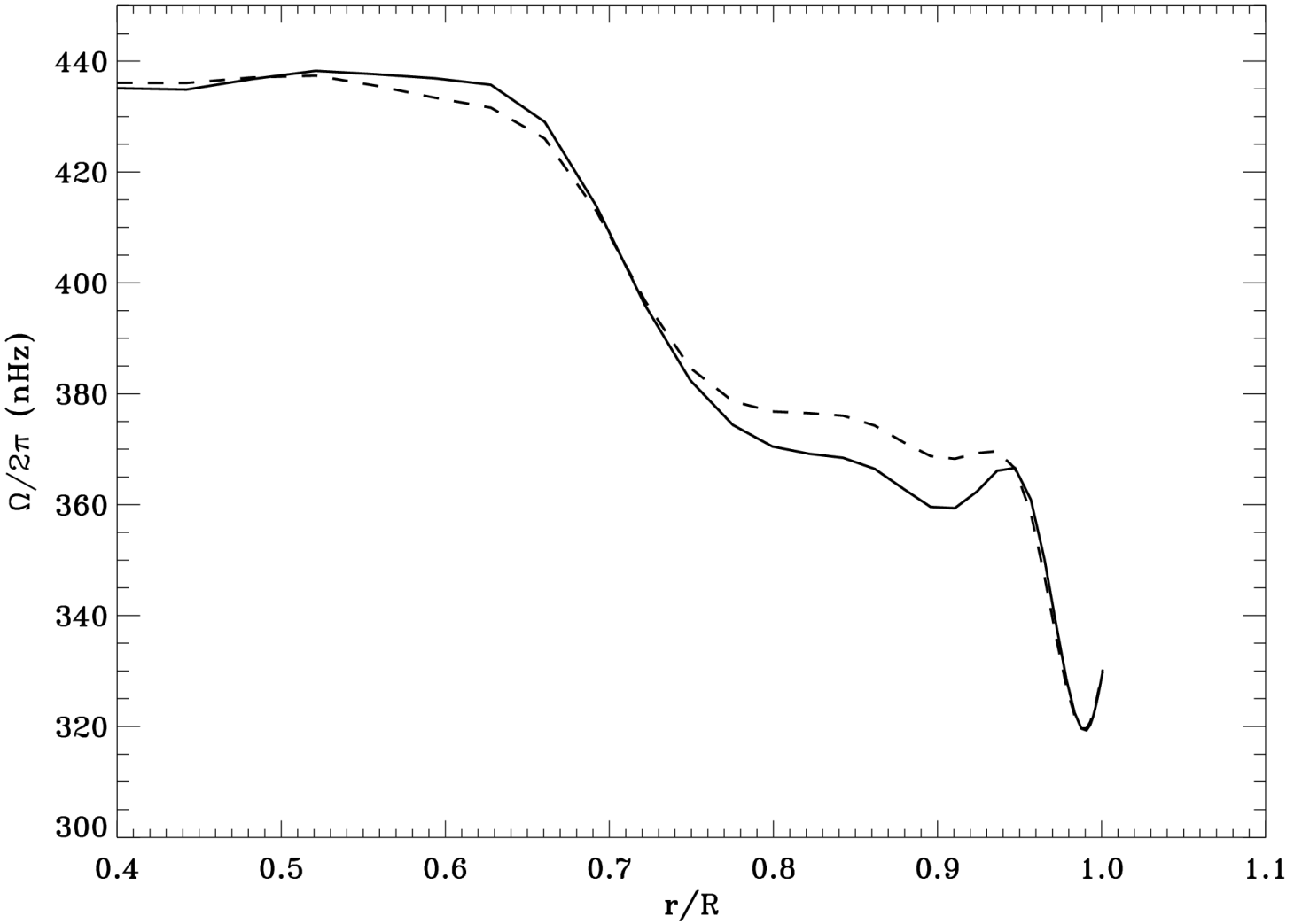

What’s Next?

- Use combination of leaks from different pixel offsets in fitting
- Account for cross terms
- Convolve with point spread functions
- Try different apodizations to get more clues
  - different apodization radii and width
  - elliptical apodization
  - apodize in latitude/longitude rather than image radius

In an attempt to quantify how our fitted mode parameters might be affected by the fact that the leakage matrix actually varies minute to minute, we computed a 72 day long timeseries of fake spherical harmonic images for several modes with the same image parameters as the actual data beginning on 2007.10.07. We then calculated the leaks as a function of time and took the power spectrum of them. We created an artificial power spectrum based on the fits to the actual data, convolved it with the power spectrum of the leaks, and then fit a lorentzian to the result to find out how much the new fitted frequency differed from the input frequency.

The first plot below shows CRPIX1 (top line) and CRPIX2 (bottom line) as a function of time. Over the same interval the B-angle decreased monotonically from 6.4 to -1.2 degrees and the observer distance decreased monotonically from 0.99 to 0.975 AU.

The next plot shows the real (bottom lines) and imaginary (top lines) parts of the sensitivity for l=m=300 as a function of time. Next shown is the power spectrum of the sensitivity. This we convolve with a lorentzian with peak frequency 1741.71 μHz and width 1.031 μHz. In this case the frequency shift is negligible, but for other leaks it can be larger. For instance, the leak to l=300,m=298 shifted by 3.6 sigma and the width shifted by 3.4 sigma, as illustrated in the last plot. This may ultimately be insignificant as well, since these errors should be scaled by sqrt(2*l + 1) to give the error on an individual mode.

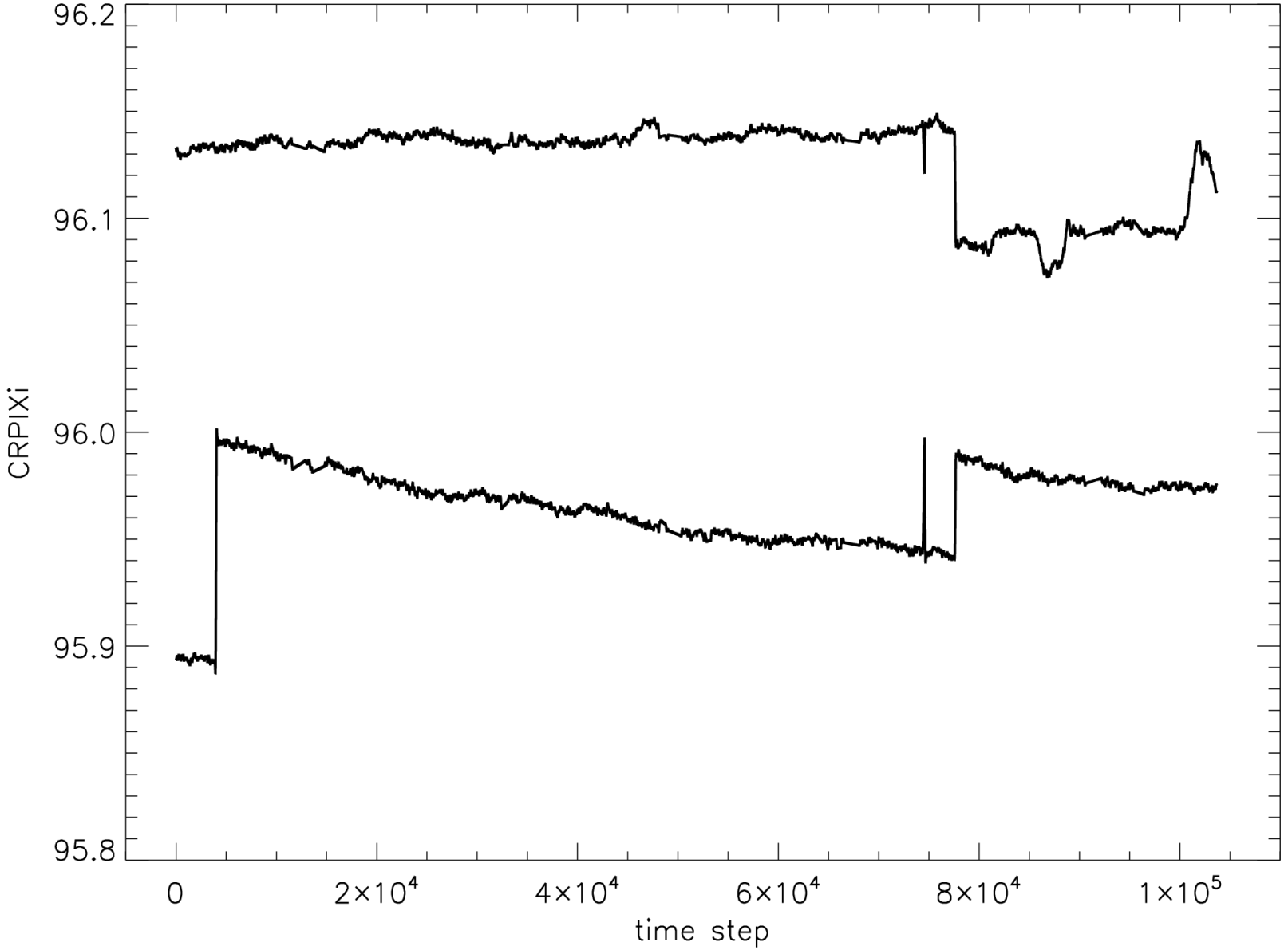
96.2
96.1
96.0
95.9
95.8
CRPIXi
0
2×10^4
4×10^4
6×10^4
8×10^4
1×10^5
time step

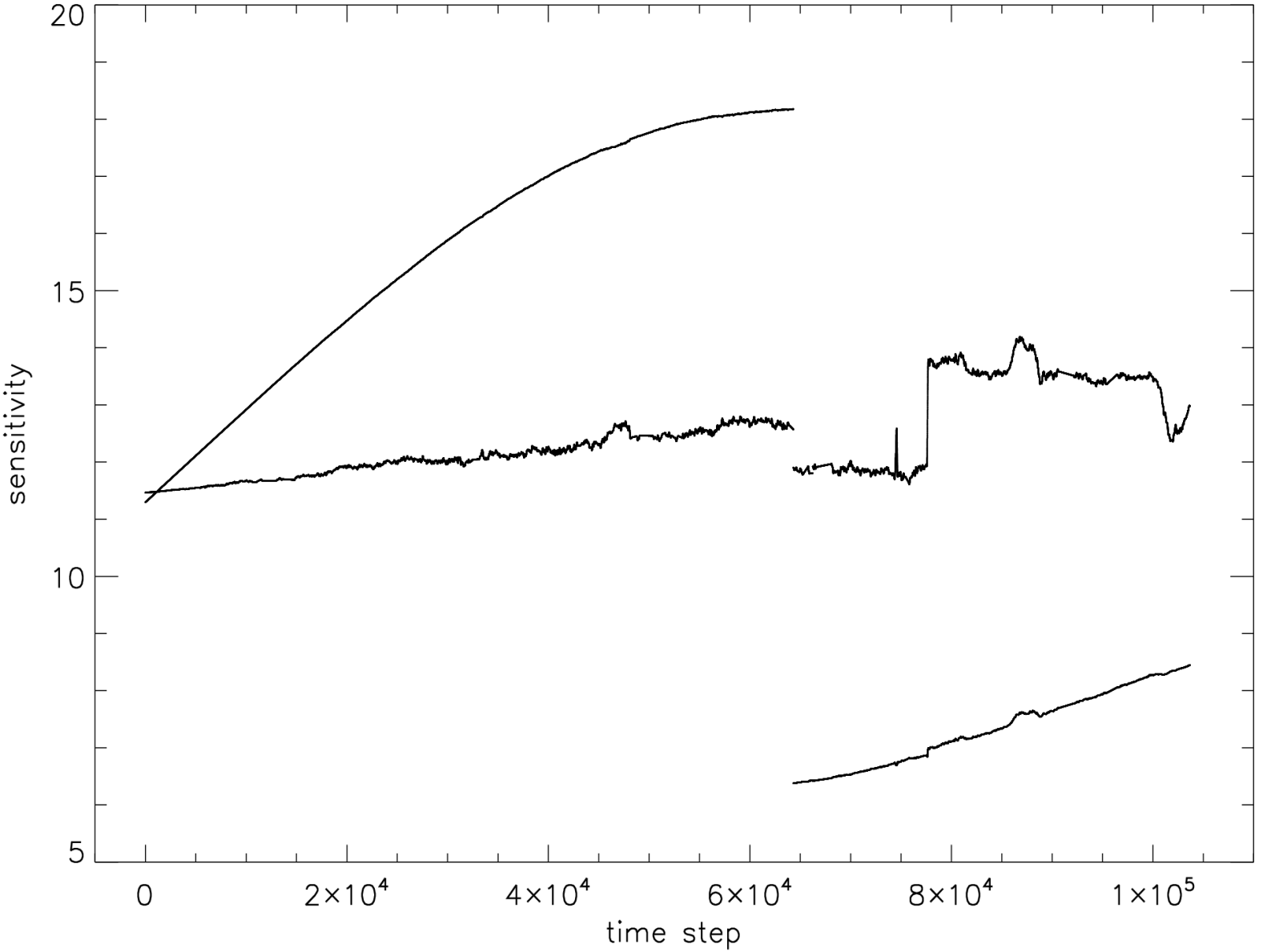
20
15
10
5
sensitivity
0
2×10^4
4×10^4
6×10^4
8×10^4
1×10^5
time step

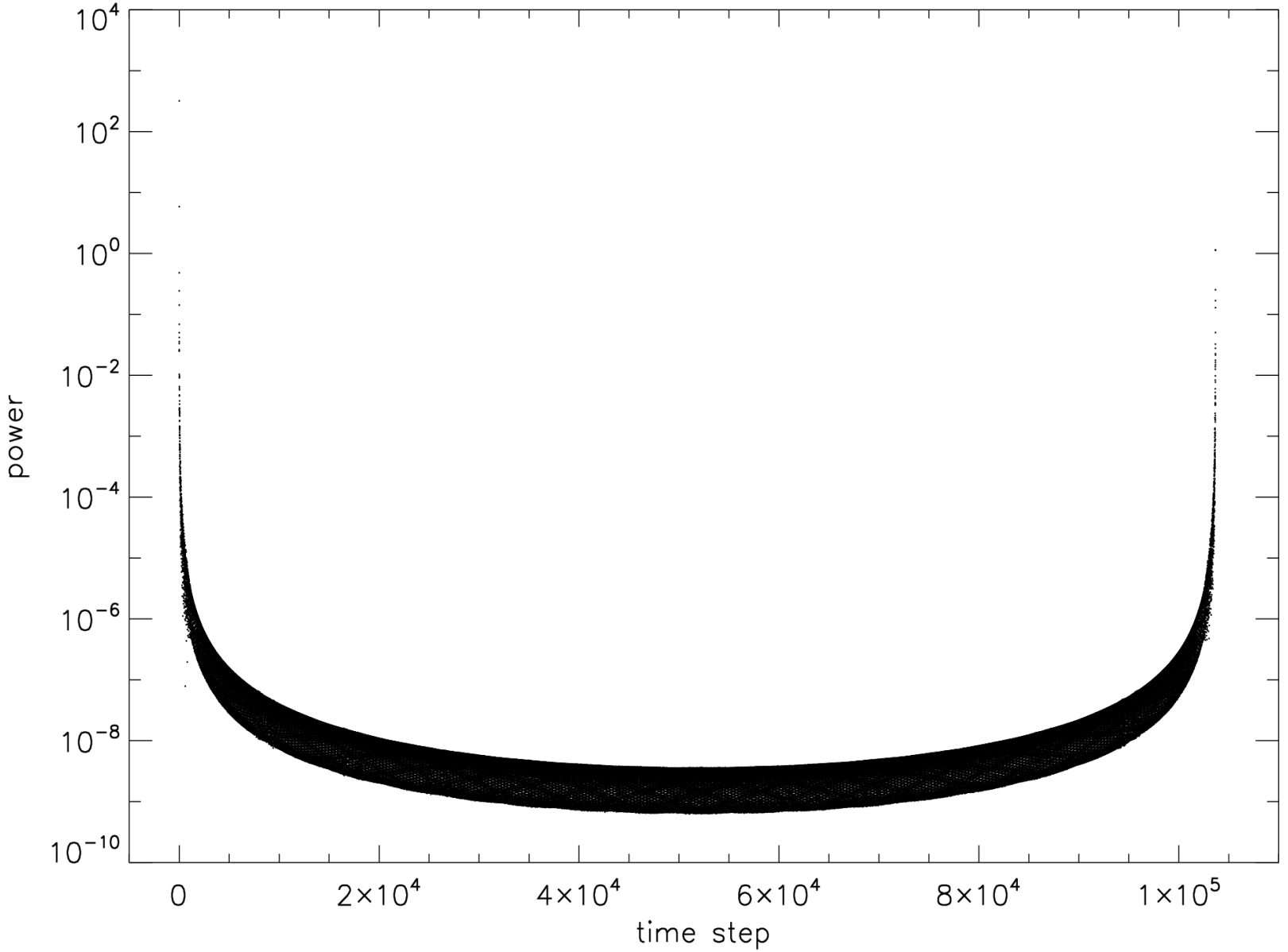
power
10^{4}
10^{2}
10^{0}
10^{-2}
10^{-4}
10^{-6}
10^{-8}
10^{-10}
0
2×10^{4}
4×10^{4}
6×10^{4}
8×10^{4}
1×10^{5}
time step

solid line: input lorentzian, dash-dot: convolved